Original Research Article

Magnetic iron oxide Fe_3O_4/α-Fe_2O_3 for Cadmium removal from aqueous solution

Comment [Y1]: Why not in capital letters and bold?

about:blank

Comment [Y2]: ?

Abstract

Magnetic iron oxide nanoparticles were successfully synthesized by co-precipitation method. The magnetite and mixture of magnetite/ hematite iron oxide were obtained and characterized by various techniques. These nanoparticles exhibited good adsorbents performance for removal cadmium metal ion. The mixture of magnetite/ hematite particles showed small size of particle and removed cadmium ion rapidly. The rates of Cd removal were 90 and 95% with Fe_3O_4 and Fe_3O_4/α-Fe_2O_3 samples respectively and the pseudo first and second kinetic models were applied to describe adsorption. Langmuir and Freundlich models were used for describing adsorption isotherms.

Keywords: iron oxide, magnetite, hematite, cadmium, heavy metal

1. Introduction

Heavy metal pollution caused by human activities became a major problem of environment and public health in our developing countries because it affects soils, plants and drinking water. The population contaminated by heavy metal such as cadmium (Cd) are exposed to diseases such as osteoporosis, cardiovascular diseases renal, gastrointestinal, neurological and cancer [1]. It is necessary to remove cadmium from wastewater or ground before contaminating population. A few methods used to remove heavy metals from the wastewater were chemical precipitation [2], ion exchange [3], membrane separation, filtration [4] and adsorption [5,6]. Among these, the adsorption technique is very cost-efficient and simple. The adsorption process consists to add adsorbents into the wastewater system and the heavy metals will be adsorbed onto the adsorbents because of the difference in the electronegative charge [7] or pore size [8]. As adsorbents, nanoparticles have gained attention due to their unique morphological and physicochemical properties such as ultra-small size, shape and size

Comment [Y3]: Erase word "our"

distribution. Iron oxide nanomaterials have demonstrated efficient adsorbents for organic dyes and heavy metal ions [9]. The magnetic nature of the iron oxide material allows fast magnetic separation after the adsorption process. Therefore, magnetic particles can be, a very good option for the adsorption of various metal ions [10]. Thus, several type of iron oxide nanoparticles and iron oxide-based nanoparticles have been used for cadmium adsorption. These adsorbents removed cadmium and showed different adsorption capacities. The magnetite-maghemite mixture oxide showed 3,6 mg/g capacity adsorption [11]. The magnetite nanoparticles and an oxide mixture of granular mullite displayed adsorption capacities of 5,5 and 2,8 mg/g respectively [12,13]. A mixture of iron oxide containing phosphorus showed adsorption capacity of 13,5 mg/g [14]. The shellac-coated iron oxide nanoparticles showed cadmium removal capacity of 18,8 mg/g [15]. Maghemite associated with bacteria was prepared as the material and showed adsorption capacity of 33,6 mg/g [16] of cadmium. The aim of this present work was to investigate the adsorption capacity of magnetite and magnetite/hematite magnetic iron oxides for the removal of cadmium from aqueous solution. The physical and chemical characteristics of synthesized iron oxide were determined using several analysis methods.

2. Material and methods

2.1 Synthesis

The synthesis method was described before in our previous paper. The amounts of 1,41 and 2,76 g of $FeSO_4$, $7H_2O$ and $FeCl_3$, $6H_2O$ respectively were mixed in 180 ml of deionized water under stirring (molar ration Fe^{2+}/Fe^{3+} =1/2). The black precipitate was obtained when amounts of precipitating agents were added such 4M of ammonium hydroxide (NH_4OH), sodium hydroxide (NaOH), solutions. The precipitates were recovered, washed several times with deionized water until pH 7 and then dried at 70°C overnight.

2.2 Cadmium adsorption experiments

Kinetic study of cadmium adsorption was carried out with the initial concentration of cadmium solution adjusted to 10 mg/L and the optimal pH was 6,3. The iron oxide synthesized nanoparticles were added to the cadmium solution and placed in a shaker for adsorption reaction. The adsorption reaction was finished at 120 min.

Isotherm adsorption experiments were conducted by mixing 0,1 g of the synthesized iron oxides with 25 mL of cadmium solution in 100 mL vials at room temperature. The metal solutions varied from 1 to 16 mg/L prepared by dissolving $Cd(NO_3)_2$ in an amount of deionized water and the initial pH of cadmium solution was adjusted to 6,3. After the

Comment [Y4]: 6.3

Comment [Y5]: 6.3

adsorption reaction, the aqueous solution were filtered through the 0.45 μm syringe filter, and the concentration of cadmium in the sample was tested by atomic absorption (spectr AA20).The amount of heavy metals or cadmium adsorbed per unit weight of iron oxide nanoparticles (Qe, mg/g) was calculated using the following equation:

$$Q_e = \frac{(C_0 - C_e)V}{m} \quad (1)$$

where C_0 and C_e represent the initial and equilibrium concentrations (mg/L) of the cadmium metal ions in the solution. V is the aqueous solution volume (L) and m is the mass (g) of the iron oxide materials.

The pseudo-first-order and pseudo-second-order kinetic models were used to fit the adsorption curves. The pseudo-first-order kinetic equation [17]:

$$\ln(q_e - q_t) = \ln(q_e) - k_1 t \quad (2)$$

where, k_1 is rate constant (min^{-1}), qt is adsorption capacity (mg g^{-1}), and q_e is equilibrium adsorption capacity (mg g^{-1}).

Comment [Y6]: Consistent with above with mg/g

The pseudo-second-order kinetic equation [18]:

$$\frac{1}{q_t} = \frac{1}{k_2 q_e^2} \times \frac{1}{t} + \frac{1}{q_e} \quad (3)$$

where, k_2 is rate constant (g mg^{-1} min^{-1}), qt is adsorption capacity (mg g^{-1}), and q_e is equilibrium adsorption capacity (mg g^{-1}).

Langmuir and Freundlich models, were used for describing adsorption isotherms. The Langmuir isotherm model is defined as Eq. (5) [19], while the Freundlich isotherm model is given in Eq. (6) [20]

$$\frac{C_e}{q_e} = \frac{1}{q_{max}} C_e + \frac{1}{K_L q_{max}} \quad (5)$$

Where, *Ce* is equilibrium concentration (mg $^{-1}$), q_e is equilibrium adsorption capacity (mg g^{-1}), q_{max} is maximal adsorption capacity (mg g^{-1}), and K_L is adsorption constant.

Freundlich adsorption isotherm is:

$$log q_e = log K_F + \frac{1}{n} log C_e \quad (6)$$

Where, C_e is equilibrium concentration (mg $^{-1}$), q_e is equilibrium adsorption capacity (mg g^{-1}), and K_F and *n* are adsorption constants.

2.3 Characterization

XRD patterns were obtained using a Bruker D8 powder (XRD) instrument employing CuKα radiation (λ =1,5418 Å). The iron oxide nanoparticles were further characterized using a

Scanning Electron Microscopy (SEM) by using JOEL JEM-2100F model with a 200 keV. Nitrogen gas adsorption measurements were performed at -196°C by using an micromeritics tristar II plus instrument. A vibrating sample magnetometer (VSM, Lakeshore, model 7400 series) was used at room temperature and the magnetic response was studied using a squid magnetometer (MPMS, Evercool, 7 T Squid instrument supplied by Quantum Design).

3. Results and discussion

3.1 Characterization

Fig 1 shows XRD patterns of synthesized iron oxide nanoparticles. XRD patterns of synthesized particles were compared with the standard diffraction spectra (JCPDS: 19-0629), and (JCPDS 33-0664). The synthesized iron oxide obtained using NH_4OH showed magnetite particles (Fe_3O_4) and iron oxide obtained using NaOH showed mixture of magnetite/hematite particles (Fe_3O_4/α-Fe_2O_3). Fig. 2 shows the scanning electron microscopy images of the different samples. Spherical particles are obtained and are uniform for magnetite and magnetite/hematite mixture. However, magnetite particles showed a strong agglomeration of the particles comparatively to the magnetite/hematite mixture. Fig. 3 shows the hysteresis plots of the magnetic iron oxides synthesized. The hysteresis-free magnetization curve indicating that magnetite and magnetite/hematite mixture were superparamagnetic. The magnetization strength were 58 and 75 emu/g for the Fe_3O_4/α-Fe_2O_3, and Fe_3O_4 respectively.

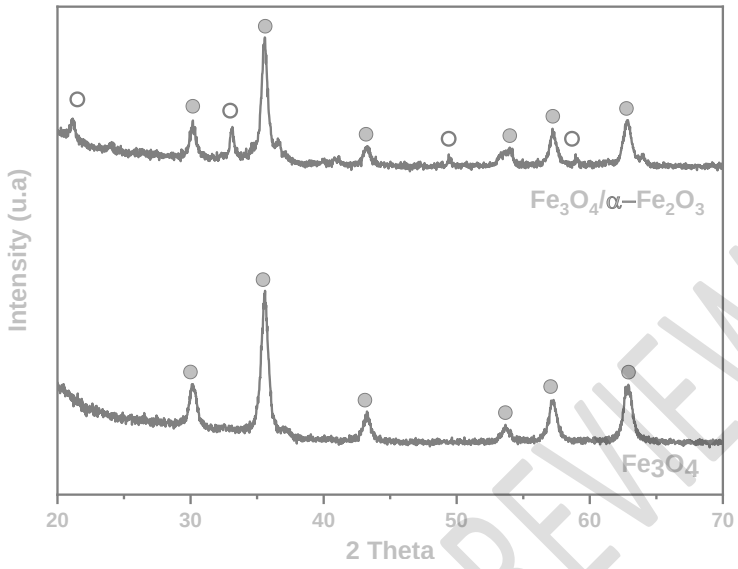

Fig. 1: XRD patterns of Fe_3O_4 and Fe_3O_4/Fe_2O_3

This result confirmed the strong particles aggregation observed in SEM for the magnetite sample (Fig. 2). Table 1 shows the results of the nitrogen adsorption isotherms at -196 °C for the iron oxide nanoparticles. The surface areas obtained were 113 and 84 m^2/g for the mixture Fe_3O_4/α-Fe_2O_3, and Fe_3O_4 respectively. The surface area obtained depended of the precipitating agent used. High surface area is generally generated by small size of particles. The sample containing Fe_3O_4 particles therefore, showed much larger particle sizes than the mixture Fe_3O_4/α-Fe_2O_3, which confirmed the aggregation of the particles. The size of the particles estimated using the Sherrer's equation [21] and the peaks of the XRD were showed in table 1 and revealed different size of particles in agreement with BET results.

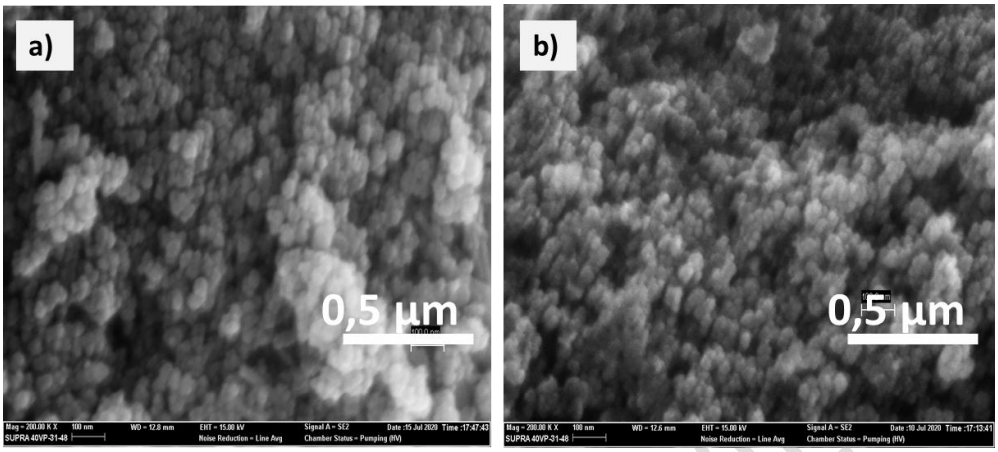

Fig 2: SEM image of a) Fe_3O_4 and b) Fe_3O_4/α-Fe_2O_3 nanoparticles synthesized

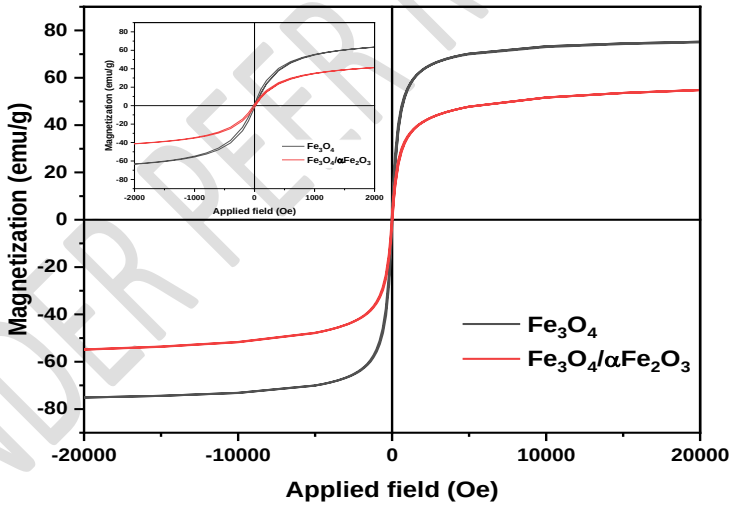

Fig.3: The hysteresis plots of magnetite–hematite mixtures and magnetite synthesized.

Comment [Y7]: Where is your explanation for Fig 3?

Table 1; Proprieties, size of particles and results of nitrogen gas adsorption measurements

Comment [Y8]: Properties

adsorbents	Magnetic saturation (emu/g)	Surface area S_{BET} (m^2/g)	Pore volume (cm^3/g)	Particle size (nm) from DRX
Fe_3O_4	75	84	0,210	13,2
Fe_3O_4/α-Fe_2O_3	58	113	0,235	8

3.2 Kinetic study

The kinetic study of Cd adsorption was carried out on Fe_3O_4/α-Fe_2O_3, and Fe_3O_4 particles. The amount removal rate increased with contact time and exhibited a rapid stage in the first 15 min for both iron oxides. Afterwards, removal rates increased and reached to saturation after 35 min. This short contact time is due to the low pore volume of the materials and surface area observed (Table 1). The rates of Cd removal were 90 and 95% with Fe_3O_4 and Fe_3O_4/α-Fe_2O_3 samples respectively at the equilibrium time. Furthermore, in order to explore the adsorption process and describe the kinetic model of cadmium adsorption, the first and second order kinetic models were applied. The cadmium adsorption kinetic data were fitted by these models. The fitting plots of pseudo-first-order and pseudo-second-order models are presented in Fig. 5. The values correlation coefficients obtained from the fitting plots were also presented in Table 2.

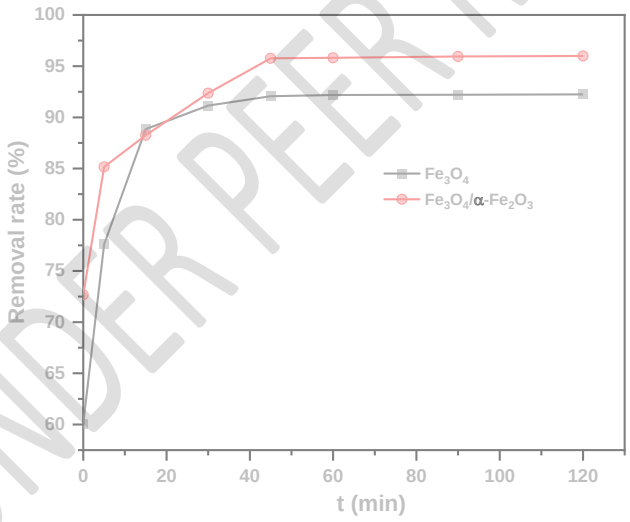

Fig 4. : The effect of contact time on the adsorption capacity of the magnetite and magnetite–hematite mixture, for cadmium (II), pH 6,3 and initial metal ion concentration of 10 mg/g

Comment [Y9]: There is not explanation for Fig.4

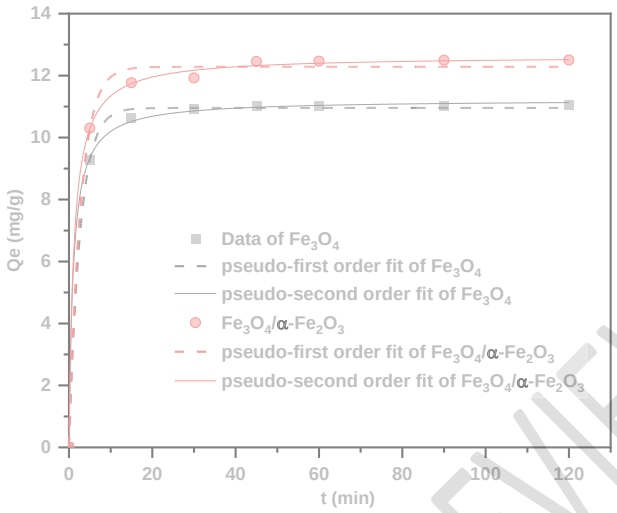

Fig. 5 : Kinetic models of pseudo-first-and second order adsorption fitting curves

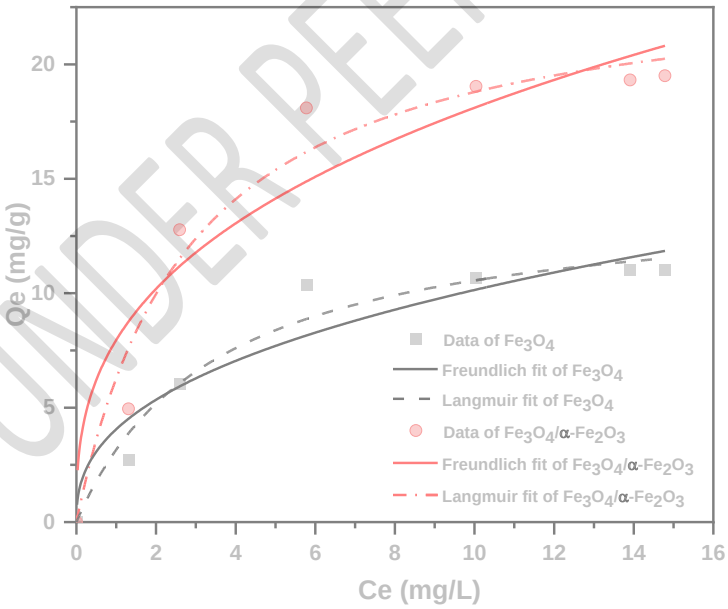

Fig 6 : Langmuir and Freundlich adsorption isotherms fitting curves

Table 2: Kinetic parameters and Langmuir and Freundlich parameters obtained for the adsorption of cadmium on Fe_3O_4 and Fe_3O_4/α-

Adsorbents	Fe_3O_4					Fe_3O_4/α-Fe_2O_3				
Kinetic models parameters	Qe, exp (mg/L)	Qe, th (mg/L)	K_1. (Min^{-1})	K_2 min (g/mg)	R^2	Qe, exp (mg/L)	Qe, th (mg/L)	K_1. (Min^{-1})	K_2 min (g/mg)	R^2
Pseudo-first order	11,04	10,95	0,3741	_	0,998	12,50	12,28	0,3610	_	0,995
Pseudo-second order	11,04	11,22	_	0,0887	0,999	12,50	12,63	_	0,0693	0,999
Isotherms models parameters	Q_m	K_L	K_F	n	R^2	Qm	K_L	K_F	n	R^2
Langmuir	14,5	0,2855	-	_	0,96	24,13	0,3516	_	_	0,95
Freundlich	_	_	4,05	0,39	0,80	_	_	7,95	0,37	0,76

We observed from the values of correlation coefficients that the pseudo-second-order kinetic model fitted well as compared to first-order model. The kinetics of Cd (II) adsorption process obeyed second-order kinetics. It indicated that the adsorption behaviour of Fe_3O_4 and Fe_3O_4/α-Fe_2O_3 respectively for cadmium was mainly dominated by chemical adsorption [22].

3.3 Isotherms

In order to determine the maximum adsorption capacities of cadmium on Fe_3O_4 and Fe_3O_4/α-Fe_2O_3 samples respectively, the isotherms were studied. The results were showed in Fig.6 where cadmium adsorption isotherms and the simulations with the Langmuir and Freundlich equations were fitted. The corresponding parameters are summarized in Table 2. The maximum cadmium adsorption capacities were 11,04 and 19,5 mg/g on Fe_3O_4 and Fe_3O_4/α-Fe_2O_3 samples respectively. The mixture Fe_3O_4/α-Fe_2O_3 showed the highest cadmium removal capacity. This result can be explained by the small size of particle and high surface area for the Fe_3O_4/α-Fe_2O_3 sample comparatively to Fe_3O_4. The fitting parameters in Table 2 indicated the adsorption processes of cadmium by the Fe_3O_4 and Fe_3O_4/α-Fe_2O_3 samples respectively obeyed to the Langmuir model well ($R^2 \geq 0,95$), representing the monolayer adsorption. The saturated adsorption capacities of Fe_3O_4 and Fe_3O_4/α-Fe_2O_3 are superior to others magnetic based material adsorbents materials as shown in table 3. The mixture magnetite/hematite (Fe_3O_4/α-Fe_2O_3) material demonstrated the most abilities to remove cadmium ion.

Comment [Y10]: Table 3

Table 3: Comparison of cadmium adsorption capacities with various iron oxide materials.

Iron oxide	Q_{max}	References
Iron oxide nanoparticles	18,32 mg/g	[1]
Maghemite/bacteria	33,6 mg/g	[14]
Iron oxide/mullite granular	2,8 mg/g	[13]
Fe_3O_4-$FePO_4$	13,5 mg/g	[23]
Magnetite nanoparticle	5,5 mg/g	[12]
Shellac-coated iron oxide	18,8 mg/g	[11]
Magnetite/maghemite	3,6 mg/g	[24]
Magnetite/hematite	19,5 mg/g	Our study

magnetite	11 mg/g	Our study

4. Conclusion

In this study, the resulting iron oxide adsorbents synthesized by co-precipitation with different precipitating agents (NH_4OH, NaOH) displayed Fe_3O_4 and Fe_3O_4/α-Fe_2O_3 particles respectively. These materials were in nanosized and exhibited surperparamgnetic proprieties and were demonstrated excellent adsorption performances for cadmium. The mixture Fe_3O_4/α-Fe_2O_3 had the strong affinity to remove cadmium comparatively to Fe_3O_4. The results of this work can give guidance for developing cost-effective adsorbents based magnetic iron oxide for heavy removal.

Comment [Y11]: superparamagnetic

References

[1] R. Bhateria, R. Singh, A review on nanotechnological application of magnetic iron oxides for heavy metal removal, J. Water Process Eng. 31 (2019) 100845.

[2] Q. Chen, Y. Yao, X. Li, J. Lu, J. Zhou, Z. Huang, Comparison of heavy metal removals from aqueous solutions by chemical precipitation and characteristics of precipitates, J. Water Process Eng. 26 (2018) 289–300.

[3] A. Bashir, L.A. Malik, S. Ahad, T. Manzoor, M.A. Bhat, G.N. Dar, A.H. Pandith, Removal of heavy metal ions from aqueous system by ion-exchange and biosorption methods, Environ. Chem. Lett. 2018 172. 17 (2018) 729–754.

[4] T.S. Vo, M.M. Hossain, H.M. Jeong, K. Kim, Heavy metal removal applications using adsorptive membranes, Nano Converg. 2020 71. 7 (2020) 1–26.

[5] S. Rajendran, A.K. Priya, P. Senthil Kumar, T.K.A. Hoang, K. Sekar, K.Y. Chong, K.S. Khoo, H.S. Ng, P.L. Show, A critical and recent developments on adsorption technique for removal of heavy metals from wastewater-A review, Chemosphere. 303 (2022) 135146.

[6] C. Xu, Y. Feng, H. Li, R. Wu, J. Ju, S. Liu, Y. Yang, B. Wang, Adsorption of heavy metal ions by iron tailings: Behavior, mechanism, evaluation and new perspectives, J. Clean. Prod. 344 (2022) 131065.

[7] J.P. Ruparelia, S.P. Duttagupta, A.K. Chatterjee, S. Mukherji, Potential of carbon

nanomaterials for removal of heavy metals from water, Desalination. 232 (2008) 145–156.

[8] A.S. Ello, L.K.C. De Souza, A. Trokourey, M. Jaroniec, Development of microporous carbons for CO2 capture by KOH activation of African palm shells, J. CO2 Util. 2 (2013).

[9] E.T. Liu, H. Zhao, H. Li, G. Li, Y. Liu, R. Chen, Hydrothermal synthesis of porous α-Fe2O3 nanostructures for highly efficient Cr(VI) removal, New J. Chem. 38 (2014) 2911–2916.

[10] M. Khosravi, S. Azizian, Adsorption of anionic dyes from aqueous solution by iron oxide nanospheres, J. Ind. Eng. Chem. 20 (2014) 2561–2567.

[11] T. Pradeep, Anshup, Noble metal nanoparticles for water purification: A critical review, Thin Solid Films. 517 (2009) 6441–6478.

[12] A.R. Mahdavian, M.A.S. Mirrahimi, Efficient separation of heavy metal cations by anchoring polyacrylic acid on superparamagnetic magnetite nanoparticles through surface modification, Chem. Eng. J. 159 (2010) 264–271.

[13] Q. Zhou, T. Long, J. He, J. Guo, J. Gao, Cadmium removal from water by enhanced adsorption on iron-embedded granular acicular mullite ceramic network, J. Taiwan Inst. Chem. Eng. 106 (2020) 92–98.

[14] X. Liang, G. Wei, J. Xiong, F. Tan, H. He, C. Qu, H. Yin, J. Zhu, R. Zhu, Z. Qin, J. Zhang, Adsorption isotherm, mechanism, and geometry of Pb(II) on magnetites substituted with transition metals, Chem. Geol. 470 (2017) 132–140.

[15] J. Gong, L. Chen, G. Zeng, F. Long, J. Deng, Q. Niu, X. He, Shellac-coated iron oxide nanoparticles for removal of cadmium(II) ions from aqueous solution, J. Environ. Sci. 24 (2012) 1165–1173..

[16] T. Mahmood, M.T. Saddique, A. Naeem, S. Mustafa, N. Zeb, K.H. Shah, M. Waseem, Kinetic and thermodynamic study of Cd(II), Co(II) and Zn(II) adsorption from aqueous solution by NiO, Chem. Eng. J. 171 (2011) 935–940.

[17] E.D. Revellame, D.L. Fortela, W. Sharp, R. Hernandez, M.E. Zappi, Adsorption kinetic modeling using pseudo-first order and pseudo-second order rate laws: A review, Clean. Eng. Technol. 1 (2020) 100032.

[18] J.C. Bullen, S. Saleesongsom, K. Gallagher, D.J. Weiss, A Revised Pseudo-Second-Order Kinetic Model for Adsorption, Sensitive to Changes in Adsorbate and Adsorbent Concentrations, Langmuir. 37 (2021) 3189–3201.

[19] X. Guo, J. Wang, Comparison of linearization methods for modeling the Langmuir adsorption isotherm, J. Mol. Liq. 296 (2019) 111850.

[20] K. Walsh, S. Mayer, D. Rehmann, T. Hofmann, K. Glas, Equilibrium data and its analysis with the Freundlich model in the adsorption of arsenic(V) on granular ferric hydroxide, Sep. Purif. Technol. 243 (2020) 116704.

[21] S. Thomas, N. Kalarikkal, A.R. Abraham, Design, fabrication and characterization of multifunctional nanomaterials, Elsevier, 2022.

[22] P. Liu, D. Rao, L. Zou, Y. Teng, H. Yu, Capacity and potential mechanisms of Cd(II) adsorption from aqueous solution by blue algae-derived biochars, Sci. Total Environ. 767 (2021) 145447.

[23] L.P. Lingamdinne, J.R. Koduru, R.R. Karri, Green synthesis of iron oxide nanoparticles for lead removal from aqueous solutions, Key Eng. Mater. 805 KEM (2019) 122–127.

[24] S.R. Chowdhury, E.K. Yanful, Arsenic and chromium removal by mixed magnetite–maghemite nanoparticles and the effect of phosphate on removal, J. Environ. Manage. 91 (2010) 2238–2247.